Phosphorus NMR and *ab initio* study of pentaphosphorus dichalcogenide halides †

Bruce W. Tattershall,*[a] **Roger Blachnik** *[b] **and Alexander Hepp** *[b]*

[a] Department of Chemistry, University of Newcastle, Newcastle upon Tyne, UK NE1 7RU
*[b] Institut für Chemie, Universität Osnabrück, D-49069 Osnabrück, Germany*

All twelve molecules $P_5S_nSe_{2-n}X$ ($n = 0$–2, X = Cl, Br or I) have been identified by ^{31}P NMR spectroscopy in mixtures in solution, obtained after thermal reactions of red phosphorus, chalcogens, and phosphorus trihalides. *Ab initio* geometries of eight of the molecules (X = Cl or Br) have been calculated, and deformations of the cages from C_s symmetry ascribed to non-bonded intramolecular interactions. Gauge including atomic orbitals (GIAO) calculation, at an economical level, of changes in ^{31}P NMR shieldings on formal atom replacement, has been shown to be a practical method for assignment of NMR spectra and hence identification of these compounds. Approximate calculation of differences in [31]P–[31]P coupling constants, using Natural Bond Orbital analysis and McConnell's equation, provided supporting evidence.

Introduction

The iodide P_5S_2I **1** may be made as a mixture with α-$P_4S_3I_2$ **2**, P_4S_3 and phosphorus iodides by high-temperature reaction of the elements,[1] and derivatives P_5S_2X may be made from it by replacement of iodine. It also occurs as a minor product, along with $P_5S_2Bu^t$, in the light-induced reaction of P_4S_3 with Bu^{t}I; other compounds P_5S_2R, where R is organic, can be made by thermal reaction of P_4S_3 with RI.[2] In recent work we have examined the effect on ^{31}P NMR chemical shifts and coupling constants of replacement of sulfur by selenium in α-$P_4E_3I_2$ **2**,[3] β-$P_4E_3I_2$ **3**,[4] β-$P_4E_3(I)CHI_2$ **3**,[5] and $P_3E_2Se_2X$ **4** (X = Cl, Br or I),[6]
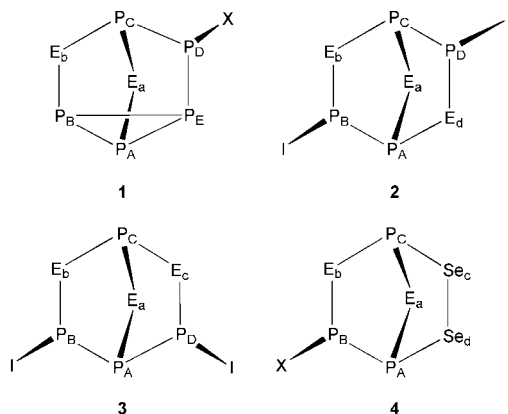
where E represents S or Se. The work has allowed considerable insight into the control of the NMR parameters by molecular geometry. One factor which has emerged has been interaction of the exocyclic, ligand atom or group with the chalcogen atoms in the bicyclic structures.

In all of the systems **2**–**4**, the primary reason for non-equivalence of sites for chalcogen substitution is inherent in the connectivity of the skeleton (*e.g.* the non-equivalence of sites

E_a and E_b in α-$P_4E_3I_2$ **2**) or results from unsymmetric ligand substitution (sites E_b and E_c in β-$P_4E_3(I)CHI_2$ **3**). Molecules P_5E_2X **1** are interesting because here the sites E_a and E_b are non-equivalent not because of different connectivity, but only because the ligand X attached to pyramidal phosphorus atom P_D points in the direction of E_a and away from E_b, and the lone pair of electrons on P_D points towards E_b rather than E_a. Investigation of the effects of endocyclic selenium substitution in molecules P_5S_2X, along with the effects of exocyclic halogen substitution, would provide therefore an opportunity of isolating one of the several factors which influence relative isomer stability, as well as ^{31}P NMR parameters of these fused ring systems. The closed nature of the P_5E_2 cage also offers the advantage of reducing to a more comprehensible level the number of possibilities for geometric change consequent upon replacement of sulfur by selenium, aiding the rationalisation of changes in the NMR parameters.

We have found that P_5Se_2I can be made in the same way as its sulfur analogue, by high temperature reaction of the elements, and that use of a mixture of sulfur and selenium gives also both possible isomers of P_5SSeI, but we now report that the use of phosphorus trihalides as sources of halogen gives generally the best methods for making, in sufficient concentrations for study by ^{31}P NMR, the whole series of twelve molecules P_5E_2X, where X = Cl, Br or I, and E_2 represents all four permutations of S and Se in the chalcogen positions E_a and E_b. All phosphorus chemical shifts and [31]P–[31]P coupling constants have been measured. It has not been possible so far to obtain ^{77}Se NMR spectra, nor [77]Se satellites in the ^{31}P spectra of sufficient intensity for satisfactory analysis.

To provide information on changes of molecular geometry on chalcogen or halogen substitution, we have calculated the geometries of the eight molecules P_5E_2X (X = Cl or Br) by *ab initio* methods, and have used the gauge including atomic orbitals (GIAO) method at an economical level of calculation as a means of predicting the directions of change of ^{31}P NMR chemical shifts with these substitutions. We now report that this allowed certain assignment of the spectrum of each P_5E_2X molecule in the product mixtures, as an alternative to comparison of NMR parameters with those of related molecules [$P_4E_3X_2$ **2**, **3** or $P_3E_2Se_2X$ **4**] and use of empirical relationships

Table 1 Relative concentrations of products of types P_4E_3 or P_5E_2X, starting from atomic ratio S:Se = 1:1

X	Eqn.	Relative to:	P_4S_3	P_4S_2Se	P_4SSe_2	P_4Se_3	P_5S_2X	$P_5S_aSe_bX$	$P_5Se_aS_bX$	P_5SSeX both isomers	P_5Se_2X
I	(1)	Both types	24	40	23	3.9	2.1	3.3	0.96	4.2	1.9
		Each type	27	44	25	4.3	26	40	12	51	23
		(Stat. distrib.)^a	27	44	25	4.5	26			50	24
Br	(1)	Both types	24	41	22	4.8	2.2	2.8	0.99	3.7	2.0
		Each type	26	44	24	5.2	28	35	13	48	25
		(Stat. distrib.)^a	26	44	25	4.7	26			50	24
Cl	(2)	Both types	19	39	31	9.5	0.54	0.67	0.22	0.89	0.52
		Each type	19	40	31	9.7	28	34	11	46	27
		(Stat. distrib.)^a	18	41	33	8.5	26			50	24

^{a} Statistical distribution within each series P_4E_3 or P_5E_2X, based on the total S:Se ratio observed for products in that series.

to composition and geometry already developed. This offers a future means of identification of series of polycyclic molecules where relevant empirical knowledge has not already been built up, which is readily practicable as a routine research tool using current technology. We also show that supporting evidence for the identification could be obtained by approximate calculation of changes in ^{31}P–^{31}P coupling constants, by a method which uses only GAUSSIAN 94 software.[7]

Preparative methods

The usual method for the synthesis of phosphorus chalcogenide chlorides or bromides, by replacement of iodine in the corresponding iodides, using metalorganic or metal halides, which works well for $P_4E_3X_2$ **2** or **3**[8,9] and which is possible for P_5S_2X,[1] gave only very low yields when applied to molecules P_5E_2X containing at least one selenium atom. A further disadvantage of the halogen substitution method for making samples for ^{31}P NMR spectroscopy is that unchanged iodides complicate the interpretation of the spectra. Experiment showed that the most useful general route to P_5E_2X (X = Cl or Br) was by direct high-temperature synthesis, using the phosphorus trihalide PX_3 as the source of halogen, and that this method was also best for making P_5E_2I.

In the cases of the bromides and iodides, P_4E_3 was made first by heating the elements together, using as E only sulfur, only selenium, or a 1:1 mixture of sulfur and selenium, and was recrystallised from CS_2 before further reaction with PX_3 and red phosphorus, of which double the amount required by eqn. (1) was taken. The samples, sealed in quartz ampoules,

$$PX_3 + 2\,P_4E_3 + 6\,P \longrightarrow 3\,P_5E_2X \qquad (1)$$

were subjected to a slow heating program (see Experimental section) to allow time for reaction of volatile halides, before being annealed at 350 °C. Soluble products were extracted by long stirring with CS_2 at room temperature. Use of preformed P_4E_3, instead of taking P + E directly, gave a greater proportion of soluble products P_5E_2X (X = Br or I) and, in the mixed sulfur–selenium experiments, the ratio S:Se in these was nearer to that taken originally. In contrast, compounds P_5E_2Cl were obtained, in sufficient yields for study by NMR, only by direct reaction of the chalcogens, using the stoichiometry represented by eqn. (2). Attempts to prepare P_5ETeI (E = S or Se) or P_5Te_2I by these thermal methods failed.

$$14\,P + 6\,E + PCl_3 \longrightarrow 3\,P_5E_2Cl \qquad (2)$$
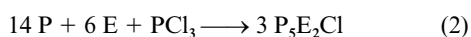
All syntheses resulted in mixtures containing the P_5E_2X compounds only in low proportion, and attempts to separate the mixtures by fractional crystallisation or HPLC were unsuccessful. Typical compositions of the solutions, measured by ^{31}P NMR integration, were: α-$P_4E_3X_2$ 30, P_4E_3 50–60, and P_5E_2X 5

mol% (X = Br or I), or α-$P_4E_3X_2$ **3**, P_4E_3 90, and P_5E_2X 2 mol% (X = Cl). The concentrations of P_5S_2X, P_5SSeX (both isomers together) and P_5Se_2X in the products approximated to statistical distributions within this series, as did the concentrations within the P_4E_3 series in the mixtures, but the ratio S:Se was higher for P_4E_3 (*e.g.* 1.81:1 in the iodides experiment starting from S:Se = 1:1) than for P_5Se_2X (1.05:1), as shown in Table 1. The loss of selenium relative to sulfur was to form insoluble, amorphous products. Of the two possible isomers $P_5S_aSe_bX$ and $P_5Se_aS_bX$, the former is thermodynamically more stable (see *ab initio* results, below) and this isomer is observed in higher concentrations, for any of the three halogens X. Similar preferences for occupation of E_a by sulfur have been observed previously in the α- or β-$P_4E_3X_2$ **2**, **3**, β-$P_4E_3(I)CHI_2$ **3**, or $P_3E_2Se_2X$ **4** series,[3–6] but now for the first time this can be attributed as due only to the smaller steric interaction between the exocyclic substituent and the chalcogen in position E_a, when this is sulfur.

Assignment of phosphorus NMR spectra

The spectra of P_5S_2X (X = Cl, Br or I) have been assigned previously,[1] and those of P_5Se_2X could be assigned by analogy, in mixtures containing no sulfur. Multiplets were assigned to one compound rather than the other, within the pairs of isomers P_5SSeX, by comparing their relative intensities and by matching coupling constants between them. Multiplets due to P_C, P_D and P_E were readily identified by the characteristic ranges of their chemical shifts and by the number of large (^1J) or small (^2J) splittings they contained. It remained to be decided which member of the pair of isomers was which, and for each isomer which multiplet belonged to P_A and which to P_B. Previous investigations of the comparable cage structures α- or β-$P_4E_3X_2$ **2**, **3**[3,4] have shown that replacement of sulfur by selenium resulted in (a) smaller positive values of the transmitted coupling $^2J_{P-E-P}$ and (b) moves of chemical shifts of both connected phosphorus atoms to lower frequency. Possible values of $^2J(P_AP_C)$ and $^2J(P_BP_C)$, and of $\delta(P_A)$ and $\delta(P_B)$, for the two isomers, were compared with corresponding values of P_5S_2X. For each halogen X, only one of the possible assignments allowed both rules (a and b) to be obeyed for replacement of sulfur by selenium at either possible position. Rules found for compounds P_5S_2R,[1] that $\delta(P_A) < \delta(P_B)$ and $^1J(P_AP_E) \geq {}^1J(P_BP_E)$, had to be abandoned for the mixed chalcogen compounds, but the assignment was confirmed by the relationship $^2J(P_AP_D) > |^2J(P_BP_D)|$, which remains true for all compounds so far discovered with the P_5E_2 skeleton. Of these ^2J couplings to P_D, $^2J(P_BP_D)$ is negative. This was assumed for previous compounds P_5S_2R by analogy with the isoelectronic $[P_7H]^{2-}$ ion,[10] but now for the first time could be demonstrated directly, for compounds $P_5S_aSe_bX$, where P_A and P_B are close enough in chemical shift, and hence the spectra are sufficiently non-first order, for relative signs of couplings to be deduced from goodness of computer

Table 2 NMR Chemical shifts and coupling constants for P_5E_2X [1]

	P_5S_2Cl	$P_5S_aSe_bCl$	$P_5Se_aS_bCl$	P_5Se_2Cl	P_5S_2Br	$P_5S_aSe_bBr$	$P_5Se_aS_bBr$	P_5Se_2Br	P_5S_2I	$P_5S_aSe_bI$	$P_5Se_aS_bI$	P_5Se_2I
$\delta(P_A)$	−70.56	−65.58	−81.64	−77.57	−70.75	−65.43	−81.89	−77.49	−72.08	−65.75	−83.10	−77.69
$\delta(P_B)$	−49.48	−64.37	−45.24	−60.23	−52.11	−66.65	−47.53	−62.13	−57.33	−70.84	−52.17	−65.75
$\delta(P_C)$	31.64	26.19	22.32	14.48	30.34	23.86	21.14	12.25	29.91	21.46	20.91	10.39
$\delta(P_D)$	199.58	206.18	208.89	215.31	169.71	176.21	179.54	185.85	111.35	119.57	122.70	130.96
$\delta(P_E)$	−212.59	−198.86	−203.12	−189.16	−209.11	−195.85	−200.04	−186.56	−200.24	−187.51	−191.86	−178.91
$^1J(P_A,P_B)$	−193.67(4)	−190.32(4)	−194.3(1)	−191.33(4)	−191.78(1)	−188.44(2)	−192.35(3)	−189.31(3)	−188.58(1)	−185.35(3)	−189.13(3)	−186.26(2)
$^1J(P_A,P_E)$	−168.81(4)	−173.41(4)	−169.2(1)	−173.53(4)	−169.14(1)	−174.04(6)	−169.44(3)	−174.39(3)	−169.08(3)	−173.86(3)	−169.33(3)	−174.40(2)
$^1J(P_B,P_E)$	−179.05(4)	−177.38(8)	−184.5(1)	−182.58(4)	−173.51(1)	−171.11(3)	−178.88(3)	−176.80(3)	−168.05(1)	−165.54(3)	−173.60(3)	−171.17(2)
$^1J(P_C,P_D)$	−274.87(4)	−282.14(5)	−275.9(1)	−283.38(4)	−265.21(1)	−272.74(3)	−266.12(3)	−273.65(3)	−251.52(1)	−258.96(3)	−251.73(4)	−259.10(2)
$^1J(P_D,P_E)$	−396.21(5)	−393.13(5)	−393.7(1)	−390.84(5)	−385.97(1)	−382.22(3)	−383.27(3)	−379.64(3)	−368.17(1)	−363.57(3)	−365.81(4)	−361.15(3)
$^2J(P_A,P_C)$	73.53(4)	82.72(4)	64.3(1)	72.97(4)	73.88(1)	83.16(6)	64.99(3)	73.48(3)	72.75(1)	81.77(3)	63.75(3)	71.94(2)
$^2J(P_A,P_D)$	15.33(4)	13.58(6)	21.3(1)	18.91(5)	15.86(1)	13.91(4)	22.13(4)	19.77(3)	17.03(1)	15.07(4)	23.63(4)	21.39(2)
$^2J(P_B,P_C)$	59.49(4)	50.33(9)	65.5(1)	55.30(4)	59.45(1)	50.24(3)	65.15(3)	55.12(3)	60.28(1)	50.97(3)	65.84(3)	55.85(2)
$^2J(P_B,P_D)$	−8.71(5)	−12.56(8)	−9.7(1)	−12.97(4)	−8.67(1)	−11.90(3)	−9.49(3)	−12.63(3)	−8.51(1)	−11.38(3)	−9.24(4)	−11.86(3)
$^2J(P_C,P_E)$	43.54(4)	44.12(4)	48.6(1)	49.83(4)	44.57(1)	45.21(3)	49.39(3)	50.70(3)	45.51(1)	46.50(2)	50.12(3)	51.76(2)
rms	0.10	0.09	0.24	0.10	0.03	0.07	0.07	0.07	0.03	0.06	0.07	0.05

Chemical shifts are in ppm relative to H_3PO_4–water and coupling constants are in Hz, with standard deviations (σ) given in parentheses. rms deviation in Hz is over all transitions fitted, using NUMARIT.

fits of the spectra. All spectra were fitted using the program NUMARIT,[11] and the resulting parameters were confirmed by simulation of the spectra using Win-DAISY and Win-NMR 1D.[12,13] Chemical shifts and coupling constants are given in Table 2.

Ab initio calculations

The Ahlrichs basis sets pVDZ and pTZV (triple zeta valence with Ahlrichs single d polarisation functions added)[14,15] offer two levels of restricted Hartree–Fock (RHF) calculation which we have previously found to predict very similar geometries for P_2Se_5.[16] Calculations using the Ahlrichs pVDZ basis (there called SVP) have been reported for an extensive series of polyphosphanes.[17] We used the lower pVDZ level for geometry optimisation of P_5E_2X molecules to provide atomic coordinates for our single point calculations of electron density and GIAO calculations of NMR shieldings, using the higher pTZV level. The Ahlrichs basis sets extend only up to Kr so our calculations were restricted to the eight molecules P_5E_2X with X = Cl or Br. The geometries found were confirmed as true minima, by vibrational analysis in each case.

Bond lengths, bond angles, and enough torsion angles to define the geometries, found by redundant internal coordinate optimisation at the RHF/pVDZ level, are given in Table 1 of the Supplementary Data, and energies are given in Supplementary Table 2. Files are provided in Supplementary Data for online viewing of the structures. Distortions from C_s symmetry are best seen as the non-bonded distances between atoms P_D, E_a and E_b, so these are presented here, along with bond angles, in Table 3. We note the following: (a) $P_D \cdots S_a > P_D \cdots S_b$, showing that the repulsion of S_a by halogen is greater than repulsion of S_b by the lone pair of P_D; (b) $P_D \cdots S_a$ increases more on replacement of S by Se than $P_D \cdots S_b$ does; (c) $P_D \cdots S_a$ increases at the expense of both other contacts when Br replaces Cl. Observation (b) shows that the $P_D \cdots E_b$ contact is more compressible than the $P_D \cdots E_a$ contact, even though that is longer. The electron density found by the *ab initio* calculations was analysed by the Natural Bond Orbital (NBO) method.[18] This showed that repulsions in the plane P_D, E_a, E_b could be visualised in terms of p-type lone pair orbitals on E_a and E_b overlapping each other and the P_D–Cl σ-bonding orbital or the lone pair orbital on P_D respectively. This is shown for P_5S_2Cl in Fig. 1, where it can be seen that the lone pair orbital of S_a also overlaps a chlorine lone pair orbital, increasing the repulsive interaction on the $P_D \cdots S_a$ side of the molecule. Observation (c) above shows that if the lone pair on P_D has a higher steric demand in the bromo- than in the chloro-compounds, this is more than compensated by the greater combined demand of bromine non-bonding and bonding orbitals. In going from P_5S_2Cl to P_5Se_2Cl, the ratios of the required increases in the non-bonded distances $E_a \cdots E_b$ and $E \cdots P_D$ to the increases in the bond lengths E–P_C are related to changes in the bond angles at P_C. These ratios are such that the bond angles at P_C stay practically constant, causing bond angles at E to decrease strongly and bond angles in the five-membered rings at other phosphorus atoms to increase. The extra length of P–P bonds to P_D, compared with P–S bonds, makes P_C nearer to P_A or P_B than to P_E. The extra repulsion of P_D–X for E_a compared with E_b draws P_C slightly closer to P_A than to P_B, when $E_a = E_b$, and bond angles to chalcogen are slightly greater at P_A than at P_B.

In single point RHF/pTZV calculations at RHF/pVDZ geometries the isomers $P_5S_aSe_bX$ were found to have lower RHF energy than $P_5Se_aS_bX$, by 3.29 (X = Cl) and 3.45 kJ mol^{-1} (X = Br), in accord with relative abundances observed after their thermal preparation and with the greater distortion from C_s cage symmetry caused by placing the larger selenium in cage position E_a, commented upon above.

Table 3 Selected *ab initio* geometric data for P_5E_2X **1** (X = Cl or Br)

	P_5S_2Cl	$P_5S_aSe_bCl$	$P_5Se_aS_bCl$	P_5Se_2Cl	P_5S_2Br	$P_5S_aSe_bBr$	$P_5Se_aS_bBr$	P_5Se_2Br
Bond lengths (Å)								
P_C–E_a	2.111	2.111	2.250	2.251	2.111	2.111	2.251	2.252
P_C–E_b	2.119	2.257	2.117	2.255	2.118	2.259	2.118	2.256
P_A–E_a	2.128	2.129	2.264	2.265	2.127	2.128	2.263	2.265
P_B–E_b	2.155	2.294	2.157	2.297	2.154	2.292	2.157	2.296
Bond angles (°)								
P_D–P_C–E_a	102.72	102.78	103.28	103.28	103.10	103.09	103.67	103.64
P_D–P_C–E_b	93.38	93.32	93.22	93.14	93.17	93.07	92.94	92.90
E_a–P_C–E_b	100.92	101.02	100.98	101.15	100.68	100.79	100.74	100.88
P_A–P_E–P_B	60.06	60.09	60.04	60.05	60.05	60.06	60.00	60.03
P_A–P_E–P_D	105.08	105.03	106.75	106.72	105.30	105.21	106.93	106.91
P_B–P_E–P_D	99.45	100.90	99.22	100.71	99.29	100.75	99.05	100.53
P_E–P_A–P_B	60.04	60.03	60.09	60.07	60.03	60.04	60.11	60.07
P_E–P_A–E_a	105.68	105.73	106.18	106.17	105.68	105.72	106.25	106.21
P_B–P_A–E_a	104.31	105.95	104.90	106.50	104.25	105.86	104.86	106.44
P_E–P_B–P_A	59.89	59.88	59.88	59.87	59.92	59.90	59.88	59.90
P_E–P_B–E_b	105.04	105.30	105.04	105.26	105.01	105.28	104.99	105.28
P_A–P_B–E_b	103.47	103.89	104.91	105.33	103.37	103.87	104.85	105.28
P_C–P_D–P_E	100.49	101.44	101.55	102.55	100.45	101.43	101.55	102.52
P_C–P_D–X	100.92	100.73	101.55	101.34	101.53	101.30	102.22	101.98
P_E–P_D–X	99.94	99.12	100.37	99.53	100.32	99.52	100.78	99.98
P_C–E_a–P_A	103.26	104.24	98.67	99.65	103.29	104.29	98.67	99.67
P_C–E_b–P_B	102.95	98.44	104.02	99.51	103.01	98.48	104.06	99.54
Non-bonded distances (Å)								
$P_D \cdots E_a$	3.392	3.391	3.511	3.509	3.401	3.398	3.521	3.519
$P_D \cdots E_b$	3.166	3.262	3.158	3.253	3.160	3.256	3.151	3.248
$E_a \cdots E_b$	3.262	3.373	3.370	3.480	3.256	3.368	3.366	3.475

Geometries were optimized at the RHF/Ahlrichs pVDZ level. Further bond lengths, torsion angles, charges and energies are given in Tables 1 and 2 of the Supplementary Data.
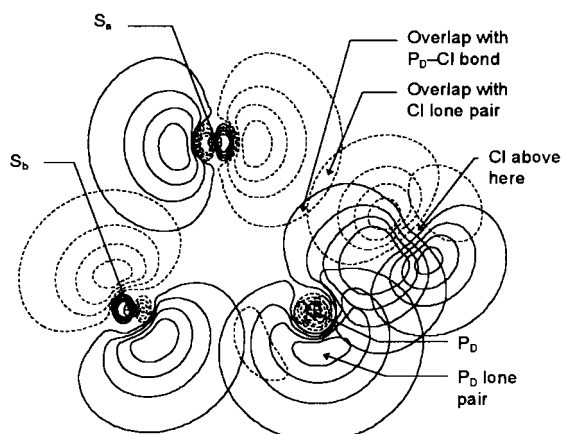
Fig. 1 Non-bonding overlaps of pre-orthogonal NBOs in the $S_aS_bP_D$ plane of P_5S_2Cl, seen from the direction of P_C.

Prediction of chemical shifts

For P_5S_2Cl with RHF/pVDZ-optimised geometry, GIAO calculations were done at RHF/pVDZ and RHF/pTZV levels and at the density functional BLYP/pVDZ, B3LYP/pVDZ and BLYP/pTZV levels. Besides this, GIAO-BLYP/pVDZ and BLYP/pTZV calculations were done using the geometry obtained by optimisation at the BLYP/pVDZ level, and GIAO-B3LYP/pVDZ on a B3LYP/pVDZ geometry. Errors of prediction of shieldings arise chiefly because (a) the level of GIAO calculation used is insufficient and (b) the calculation is for isolated gas-phase molecules and takes no account of different interactions with solvent. In principle, an empirical linear relationship between sets of observed shifts and of calculated shieldings could be fitted. In fact, at these levels of calculation, the multiplier of calculated shielding is found to be not significantly different from −1, so the problem amounts to finding the constant in eqn. (3).

$$\text{predicted shift} = \text{constant} - \text{calculated shielding} \quad (3)$$

Eqn. (4), where *n* is the number of observations, can be used to

$$\text{constant} = \frac{1}{n}(\Sigma \,(\text{observed shifts}) + \Sigma \,(\text{calculated shieldings})) \quad (4)$$

find the constant without prior assignment of chemical shifts within the investigated series. Thus, different constants can be found for different series, according to the nature of the assignment sought, eliminating some of the errors from sources (a) and (b) above.

For a single compound with several observed chemical shifts, identification can be supported and multiplets assigned to atoms, by calculating a single constant for that compound for the level of calculation used, over all observed shifts. Calculated chemical shifts for P_5S_2Cl, obtained in this way and given along with their root mean square deviations from the observed shifts in Table 4, allow comparison between the levels of calculation. While RHF/pTZV is better than RHF/pVDZ, particularly in the important task of distinguishing P_A and P_B, BLYP/pVDZ is superior to either, particularly in predicting a reasonable value for $\delta(P_C)$. The advantage is lost, however, at the BLYP/pTZV level. This may be because more sophisticated polarisation and diffuse functions are required at the higher level, which for this size of molecule would have led to impractically long calculations using our currently available computing facilities. B3LYP/pVDZ gave shieldings which fitted slightly less well than did BLYP/pVDZ. We therefore proceeded to carry out GIAO-BLYP/pVDZ calculations using RHF/pVDZ geometries for the other seven chlorides or bromides. In all cases the correlation between observed chemical shifts and calculated shieldings was better (overall Pearson $r = -0.997$) than for GIAO-RHF/pTZV ($r = -0.991$), as shown in Fig. 2. Shifts for

Table 4 Experimental and calculated chemical shifts for P_5S_2Cl

Method		Atom					
GIAO calc.	Geometry	P_A	P_B	P_C	P_D	P_E	rms deviation
Experimental:							
		−70.56	−49.48	31.64	199.58	−212.59	
Calculated:[a]							
RHF/pVDZ	RHF/pVDZ	−76.16	−71.32	51.26	184.81	−190.00	18.01
RHF/pTZV	RHF/pVDZ	−83.81	−70.99	55.01	197.28	−198.90	16.60
BLYP/pVDZ	RHF/pVDZ	−73.95	−58.53	37.32	210.44	−216.70	7.22
BLYP/pTZV	RHF/pVDZ	−82.70	−57.57	40.37	231.15	−232.64	18.37
B3LYP/pVDZ	RHF/pVDZ	−74.62	−63.46	41.30	207.32	−211.94	8.55
BLYP/pVDZ	BLYP/pVDZ	−66.31	−57.90	46.85	205.61	−229.65	11.38
BLYP/pTZV	BLYP/pVDZ	−74.84	−58.16	50.30	227.86	−246.57	21.89
B3LYP/pVDZ	B3LYP/pVDZ	−71.08	−60.27	44.76	203.34	−218.17	8.17

[a] Using one constant for the compound for each method, obtained empirically using eqn. (4).

$$\delta = 401 - 0.983\,\sigma$$

$$\delta = 281 - 0.943\,\sigma$$
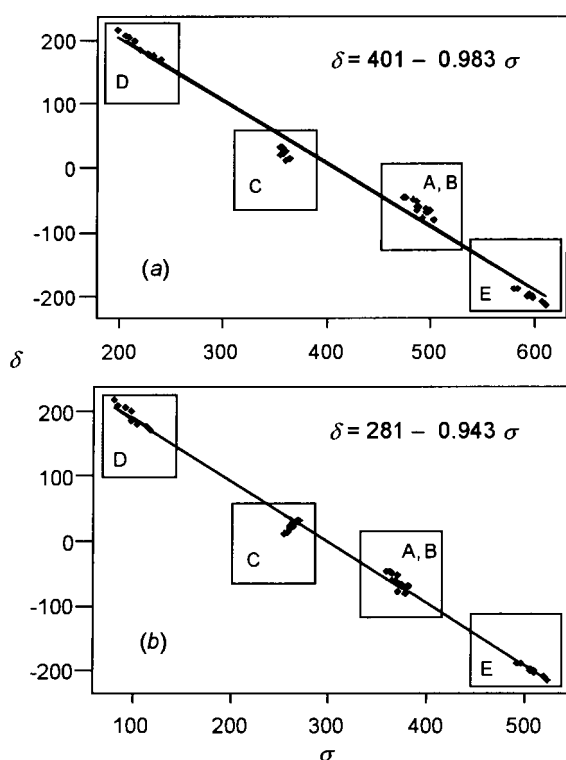
Fig. 2 Regression, for all phosphorus atoms of P_5E_2X, of observed chemical shifts on shielding calculated using (*a*) GIAO-RHF/pTZV or (*b*) GIAO-BLYP/pVDZ.

P_A and P_B were predicted to be in the order shown in Table 2, for all compounds. Individual shieldings from both levels of calculation are given in Table 3 of the Supplementary Data. As shown for P_5S_2Cl in Table 4, geometry optimisation at the BLYP/pVDZ level failed to yield better fits to the observed chemical shifts. A similar conclusion was reached for $P_5Se_aS_bCl$. We therefore have no evidence that density functional geometries are more realistic for the present molecules than Hartree–Fock geometries, for the basis sets and method we have tried, so Hartree–Fock geometries are used throughout this paper.

The presence of five non-equivalent phosphorus atoms per molecule is relatively unusual, and a potentially more useful application of eqn. (4) is to calculate a constant for a particular atom position over a series of related molecules, rather than for all atom positions within one molecule. This allows better fits than when the constant is obtained for several atom positions as well as several molecules, and in general can allow isomers, diastereomers or rotamers to be assigned to NMR signals. The present series of molecules, in which only the identities of single

atoms vary, provides a useful test of this method. If differences in observed shifts and in calculated shieldings, with stepwise replacement of sulfur by selenium or chlorine by bromine, are compared for each atom position, then the need to find constants disappears. The differences are given in Table 5, using codes for the replacements shown in Scheme 1, for both GIAO-
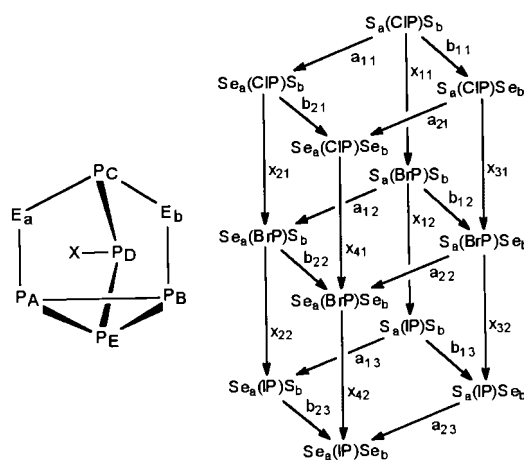
Scheme 1 Codes for formal replacements of atoms in P_5E_2X (E = S or Se; X = Cl, Br or I): replacements a_{1n} or a_{2n} of S by Se at position E_a, b_{1n} or b_{2n} at E_b; replacements x_{11}–x_{41} of Cl by Br, x_{12}–x_{42} of Br by I.

RHF/pTZV and BLYP/pVDZ calculations. At the RHF/pTZV level, the changes in shift were predicted to be in the observed directions, using the present assignment of spectra, for all atom positions and for all replacements, except for $\delta(P_C)$ under halogen replacement and for $\delta(P_A)$ in replacement x_{21} (where both observed and calculated differences were almost zero). The sizes of some of the changes were well predicted. The difference data confirm the identification of the compounds and the assignment of the spectra, without necessarily interpreting the values of coupling constants. Either observed or calculated differences in chemical shifts, on chalcogen replacements a or b, have only a small dependence on the identity of the halogen X, and differences x on halogen replacement are similar across all four S,Se skeletons. The effects of chalcogen and halogen replacement are almost independent. The table of observed differences is remarkably similar to that for β-$P_4E_3(I)CHI_2$ **3**, for which a comparable replacement scheme was presented,[5] even though those compounds do not have closed cage structures.

In contrast, the differences predicted at the BLYP/pVDZ level show a generally much poorer correspondence to observed differences, especially for phosphorus atoms adjacent to the substitution site, *e.g.* P_A in substitutions a. Only 43 out of 60

Table 5 Differences in NMR chemical shifts on atom replacement

Replacement[a]	Molecules[b]			Observed or calculated[c]	Atom				
	E_a	E_b	X		P_A	P_B	P_C	P_D	P_E
a_{11}	E	S	Cl	obs.	−11.08	4.24	−9.32	9.31	9.47
				HF	−6.86	9.61	−1.74	10.54	13.69
				DF	2.31	6.47	5.70	12.14	13.43
a_{12}	E	S	Br	obs.	−11.14	4.58	−9.20	9.83	9.07
				HF	−5.96	9.71	−0.99	11.91	13.60
				DF	2.83	6.53	6.53	13.97	13.70
a_{13}	E	S	I	obs.	−11.02	5.16	−9.00	11.35	8.38
a_{21}	E	Se	Cl	obs.	−11.99	4.14	−11.71	9.13	9.70
				HF	−6.55	9.56	−4.09	10.77	13.68
				DF	2.19	5.98	4.60	12.11	12.99
a_{22}	E	Se	Br	obs.	−12.06	4.52	−11.61	9.64	9.29
				HF	−6.42	9.98	−3.59	12.52	13.95
				DF	1.95	6.43	4.90	14.72	13.56
a_{23}	E	Se	I	obs.	−11.94	5.09	−11.07	11.39	8.60
b_{11}	S	E	Cl	obs.	4.98	−14.89	−5.45	6.60	13.73
				HF	9.97	−12.47	−2.80	6.51	13.27
				DF	7.93	−4.51	7.39	4.96	13.46
b_{12}	S	E	Br	obs.	5.32	−14.54	−6.48	6.50	13.26
				HF	10.82	−12.21	−2.71	6.45	12.97
				DF	9.01	−4.33	7.71	4.46	12.86
b_{13}	S	E	I	obs.	6.33	−13.51	−8.45	8.22	12.73
b_{21}	Se	E	Cl	obs.	4.07	−14.99	−7.84	6.42	13.96
				HF	10.28	−12.52	−5.15	6.74	13.26
				DF	7.81	−5.00	6.29	4.93	13.02
b_{22}	Se	E	Br	obs.	4.40	−14.60	−8.89	6.31	13.48
				HF	10.36	−11.94	−5.31	7.06	13.32
				DF	8.13	−4.43	6.08	5.21	12.72
b_{23}	Se	E	I	obs.	5.41	−13.58	−10.52	8.26	12.95
x_{11}	S	S	X	obs.	−0.19	−2.63	−1.30	−29.87	3.48
				HF	−0.48	−2.87	3.09	−24.25	4.01
				DF	−0.11	−4.14	2.45	−20.62	3.87
x_{12}	S	S	X	obs.	−1.33	−5.22	−0.43	−58.36	8.87
x_{21}	Se	S	X	obs.	−0.25	−2.29	−1.18	−29.35	3.08
				HF	0.42	−2.77	3.84	−22.88	3.92
				DF	0.41	−4.08	3.28	−18.79	4.14
x_{22}	Se	S	X	obs.	−1.21	−4.64	−0.23	−56.84	8.18
x_{31}	S	Se	X	obs.	0.15	−2.28	−2.33	−29.97	3.01
				HF	0.37	−2.61	3.18	−24.31	3.71
				DF	0.97	−3.96	2.77	−21.12	3.27
x_{32}	S	Se	X	obs.	−0.32	−4.19	−2.40	−56.64	8.34
x_{41}	Se	Se	X	obs.	0.08	−1.90	−2.23	−29.46	2.60
				HF	0.50	−2.19	3.68	−22.56	3.98
				DF	0.73	−3.51	3.07	−18.51	3.84
x_{42}	Se	Se	X	obs.	−0.20	−3.62	−1.86	−54.89	7.65

[a] Replacement codes defined in Scheme 1. [b] E or X represents the atom which changes in the replacement. [c] Calculated as −(difference in *ab initio* isotropic shieldings): HF = GIAO-RHF/pTZV; DF = GIAO-BLYP/pVDZ (using RHF/pVDZ geometries in both cases).

differences were predicted to be in the observed directions, compared with 55 out of 60 at the RHF/pTZV level. Differences for substitution a_{11} ($P_5Se_aS_bCl$–P_5S_2Cl), except for $\delta(P_B)$, were yet more poorly predicted if geometries optimised at the BLYP/pVDZ or B3LYP/pVDZ levels were used. We conclude that while single point calculations at a DF level deal better than RHF calculations with grossly different chemical environments, when comparing atom positions within a molecule, other errors at the DF level are less removable by taking differences between molecules. For the work on comparison of coupling constants between molecules, described below, the RHF/pTZV rather than BLYP/pVDZ calculations were used.

Prediction of coupling constants

GIAO calculations of NMR shielding are a standard procedure, although an advance presented here is to apply them to differences on atom substitution so as to eliminate part of the error. In contrast, non-empirical routes to coupling constants in heavy-atom complex molecules appear to have not yet reached a comparable popularity. An approximate calculation may be used and some unknown terms in it may be ignored, providing that the relationship between the numbers obtained and a set of

measured coupling constants is obtained statistically. As in the case of chemical shifts, the best way of eliminating unknowns is to consider changes with stepwise substitution.

Phosphorus–phosphorus couplings have been found to involve mainly the Fermi contact mechanism,[19] for which the simplest approximation is given by McConnell's eqn. (5).[20]

$$|J_{AB}| \propto P_{AB}^2 \quad \text{where} \quad P_{AB} = 2 \sum_i^{\text{occ. MOs}} c_{iA}c_{iB} \quad (5)$$

Here c_{iA} and c_{iB} are the coefficients of the valence shell s orbitals of coupled atoms A and B in molecular orbital i; P_{AB} is a density matrix element measuring the total simultaneous involvement of both atomic orbitals A and B in the total electron density. The inaccuracy inherent in this method arises because the constant of proportionality is clearly not constant, though it may be nearly so between closely related couplings. To treat a large, non-symmetric molecule, LCAO coefficients may be obtained by *ab initio* methods, but the difficulty arises of distinguishing what are valence shell s orbitals for use in McConnell's equation. We have used NBO analysis to decompose the calculated electron density into orthogonal Natural Atomic Orbitals (NAOs). The NBO program, marketed as part of the GAUSSIAN 94 software,[7,18] allows output
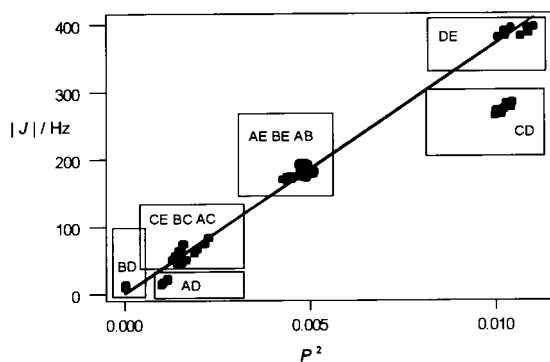
Fig. 3 Regression of $|J|$ on P^2, for all P–P couplings of P_5E_2X except $^1J(P_CP_D)$. The regression line is constrained to pass through the origin.

Fig. 4 Regression of $|^1J(P_CP_D)|$ of P_5E_2X on P^2, showing vectors for atom replacements a and b.

of the density matrix in terms of NAOs, and matrix elements P_{AB} can be selected from this for use in McConnell's equation. Using the Ahlrichs pTZV basis, as in the GIAO shielding calculations, the NBO analysis found that density matrix elements of the type P_{3sA4sB} were smaller but significant, compared with the expected elements P_{3sA3sB}. However, multiple regression of the observed P–P couplings on $P_{3sA4sB} + P_{4sA3sB}$ as well as P_{3sA3sB}, for each kind of coupling in the set of molecules P_5E_2X, showed that no significantly better predictive ability can be gained by including the P_{3sA4sB} elements than by simply taking the P_{3sA3sB} elements, usually because the sum $P_{3sA4sB} + P_{4sA3sB}$ correlated too well with P_{3sA3sB}. Similarly, for selected pairs of couplings, the sum of density elements for all pairwise combinations of 1s, 2s, 3s and 4s orbitals, on the two atoms involved in each coupling, was examined but found to give no better relative values of the couplings than by taking the P_{3sA3sB} value alone. For the coupling $^1J(P_DP_E)$ of P_5S_2Cl the composition of the sum P_{3sD3sE} was examined. It was found to include positive and negative components $c_{iD}c_{iE}$ up to 3.4 times bigger than the total. The largest 19 components out of 62 needed to be included to account for 98% of the value of P_{DE}, so, apart from the approximations implicit in using McConnell's equation, the values of P used are likely to be quite sensitive to errors in the NAO coefficients and hence to the quality of the *ab initio* calculation.

Values of P^2 obtained are shown in Table 4 of the Supplementary Data. If couplings $^1J(P_CP_D)$ were excluded, $|J|$ was found to correlate well with P^2 ($r = 0.995$), fitting a regression eqn. (6) as shown in Fig. 3. Taking each type of coupling

$$|J| = 37257\ (\sigma\ 307)\ P^2 \qquad (6)$$

separately, differences examined were smaller relative to the errors in the model, so poorer correlation was found. Deviations from the individual regression lines were systematic, such that if vectors corresponding to replacements a or b (Scheme 1) were drawn on the regression plots they formed similar quadrilaterals for chloro- and bromo-compounds, approximating to parallelograms. As an example, the plot for $^1J(P_CP_D)$ ($r = 0.749$) is shown in Fig. 4. Prediction of the relative sizes of changes on element replacement was not accurate enough to be useful, but the assignment of spectra to compounds could be supported by examining how many of these changes were predicted to be in the observed directions. We found that the calculated direction of (non-zero) changes agreed with experiment in 36/40 cases for replacements a, 32/40 for replacements b, and 28/36 for replacements x. The assignment was thus validated: in particular, the assignments of the $^2J(P_AP_C)$ and $^2J(P_BP_C)$ couplings for $P_5S_aSe_bX$ and $P_5Se_aS_bX$, and hence the identification of the P_A *versus* P_B multiplets for these compounds, were confirmed.

Intrinsically more accurate methods require at least a knowledge of energies of both occupied and virtual MOs, as well as of the coefficients of s orbitals in them. We experimented with Pople and Santry's mutual polarisability method (eqn. (7)),[21]
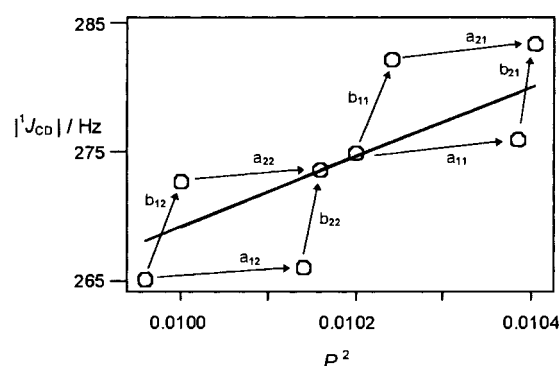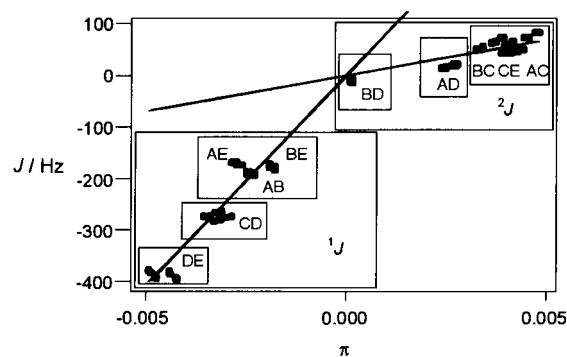

Fig. 5 Separate regression of ^1J and ^2J couplings of P_5E_2X on π. Both regression lines are constrained to pass through the origin.

$$J_{AB} \propto \pi_{AB} \text{ where } \pi_{AB} =$$
$$-4 \sum_i^{\text{occ. MOs}} \sum_j^{\text{virt. MOs}} c_{iA}c_{iB}c_{jA}c_{jB}/(\varepsilon_j - \varepsilon_i) \qquad (7)$$

using the same level of theory and using NBO analysis to obtain coefficients of 3s orbitals, as for the experiments with McConnell's method. Here ε_j and ε_i are *ab initio* energies of virtual and occupied delocalised MOs. Now, for π_{DE} of P_5S_2Cl, the largest component was 5.3 times the total, and 570 components needed to be included to accumulate 98% of the sum. This method is clearly much more sensitive to errors in the LCAO coefficients than is that based on the McConnell equation.

The values of π obtained are included in Table 4 of the Supplementary Data. While the McConnell equation yields only relative magnitudes of couplings, the Pople and Santry equation gives also their signs. These were correctly predicted for all of the present couplings, except for $^2J(P_BP_D)$, where the predicted values were almost zero. ^1J and ^2J couplings were found to fit two different regression lines on π, as shown in Fig. 5, with correlation coefficients 0.924 and 0.935, and gradients 81540 (σ 1632) and 13790 (σ 643) respectively. The cluster of points for $^1J(P_CP_D)$ was near to the regression line for all ^1J couplings, in contrast to the McConnell's equation plot, probably showing that a different 'average excitation energy' was needed for these couplings, rather than the Fermi contact mechanism being less important. Fits of individual kinds of ^2J couplings (except for $^2J(P_BP_D)$) to π were slightly better than, but very similar to, fits to P^2 in the McConnell method, while fits of individual kinds of ^1J couplings were clearly poorer. Altogether, correct directions of change were predicted in 32/40 cases for replacements a, 23/40 for replacements b, and 25/36 for replacements x. We conclude that greater susceptibility to error outweighs the greater sophistication of the Pople and Santry approach, and that the further computational effort required to accumulate π is not worthwhile.

Rationalisation of NMR parameters

The well-known 'heavy atom effect' broadly explains the moves to lower frequency of $\delta(P_D)$ on replacements x, and of $\delta(P_C)$ and $\delta(P_A)$ or $\delta(P_B)$ on replacements a or b respectively (Table 5).[22] However, increasing the endocyclic bond angle at three-co-ordinate phosphorus leads generally to a higher frequency chemical shift, so where introducing the heavier neighbour causes an increase in bond angle, this opposes the heavy atom effect. There is a bigger increase in angles at P_A on replacements a than at P_B on replacements b, and the observed (and calculated) changes in $\delta(P_A)$ are less negative than in $\delta(P_B)$. The positive changes in $\delta(P_A)$ on replacements b, of $\delta(P_B)$ on replacements a, and on $\delta(P_D)$ and $\delta(P_E)$ on replacements of either kind are all associated with increases in bond angles.

The lower chemical shift $\delta(P_A)$ than $\delta(P_B)$, when $E_a = E_b$, is contrary to bond angle arguments, and P_A and E_a are calculated to carry less electron density than P_B and E_b respectively (Table 1 of Supplementary Data), yet the GIAO calculations using the same model correctly predict that P_A is more shielded. P_E is calculated to carry a slight negative charge, which is practically unchanged on replacement of chlorine by bromine, as too is the sum of the bond angles at phosphorus, yet P_E becomes less shielded in this replacement, both in experiment and in theory.

The couplings transmitted by chalcogen, $^2J(P_AP_C)$ and $^2J(P_BP_C)$, are substantially different when $E_a = E_b$, because of the different influence of the halogen atom on the two chalcogen atoms, yet the value of each of these couplings is remarkably insensitive to the nature of the halogen. The bond angle at E_a is almost the same as that at E_b, but the bigger coupling $^2J(P_AP_C)$ seems to be associated with a shorter distance P_A–E_a than P_B–E_b, caused by the nearer approach of P_C to P_A than to P_B, described above.

Experimental

All experiments were carried out by glove-box or Schlenk techniques, under dry and O_2-free argon. CS_2 (Merck) was dried by distillation from P_4O_{10}. Purities and suppliers of reagents were: red phosphorus, 99.9999%, Knapsack; sulfur, 99.95%, Merck; grey selenium, 99.999%, ABCR; PCl_3, >99%, Strem; PBr_3, >98%, Fluka; PI_3, >99%, Merck. NMR spectra of solutions in CS_2 were measured in 5 mm diameter tubes using a Bruker AC250 spectrometer operating at 101.3 MHz for ^{31}P. Sealed capillaries containing C_6D_6 were used for locking, and chemical shifts, obtained by substitution experiments using the same capillaries, are reported relative to 85% H_3PO_4–water.

Typical experiment: preparation of a solution containing $P_5S_nSe_{2-n}Br$ ($n = 0–2$)

CAUTION: while the described procedure was designed to minimise risk, the exothermic reactions of phosphorus with chalcogens, together with the chance of generating high pressures in sealed ampoules, lead to the slight possibility of explosions. Furnaces should be suitably sited and their possible decontamination planned for.

A mixture of red phosphorus (3.10 g, 100 mmol P), sulfur (1.20 g, 37.5 mmol S) and grey selenium (2.96 g, 37.5 mmol Se) was sealed under vacuum in a glass ampoule, heated at 10 °C h^{-1} to 250 °C, and held there for two days. The cooled and crushed product was recrystallised from CS_2 to give an intermediate with average composition $P_4S_{1.4}Se_{1.6}$ (found by ^{31}P NMR integration of signals due to molecules $P_4S_nSe_{3-n}$ ($n = 0–3$) in its solution), and average molecular weight 294.9 g mol^{-1}. This material (1.59 g, 5.39 mmol) was mixed into further red phosphorus (1.00 g, 32.3 mmol P), loaded into a strong quartz glass ampoule (15 cm × 8 mm diameter), then PBr_3 (0.73 g, 2.70 mmol) added. The ampoule, sealed while containing dry argon, was heated at 10 °C h^{-1} to 350 °C, with pauses of six hours each at 120 and at 250 °C. The melt was annealed at

350 °C until it became pale orange-yellow (72 h). The cooled ampoule was opened and crushed under Ar, the resulting mass stirred with CS_2 (20 cm³) for 12 h at 21 °C, and the solution filtered to remove insoluble products and quartz fragments. Solvent was evaporated under vacuum at ambient temperature, to leave *ca.* 7 cm³ of product solution. ^{31}P NMR integration showed the solution to contain PBr_3 (15.3), α-$P_4E_3Br_2$ (29.0), P_4E_3 (50.1) and P_5E_2Br (4.3 mol%), with the P_4E_3 and P_5E_2Br components distributed as shown in Table 1. For experiments using PI_3 or PCl_3, annealing times at 350 °C were 48 and 96 h respectively. In the reaction of PCl_3 with red phosphorus and chalcogens (eqn. (2)) very slow heating to 120 °C was required on account of the volatility of PCl_3.

For the *ab initio* calculations, Ahlrichs pVDZ and TZV basis sets were obtained from the EMSL basis set database.[23] The same single d-type polarisation functions were added to the TZV set to make pTZV, as were provided in the pVDZ set.

References

1 B. W. Tattershall and N. L. Kendall, *Polyhedron*, 1994, **13**, 2629.
2 R. Blachnik, A. Hepp, P. Lönnecke, J. A. Donkin and B. W. Tattershall, *Z. Anorg. Allg. Chem.*, 1994, **620**, 1925.
3 R. Blachnik, P. Lönnecke and B. W. Tattershall, *J. Chem. Soc., Dalton Trans.*, 1992, 3105.
4 P. Lönnecke and R. Blachnik, *Z. Anorg. Allg. Chem.*, 1993, **619**, 1257.
5 B. W. Tattershall, R. Blachnik and A. Hepp, *Polyhedron*, 1995, **14**, 1779.
6 P. Lönnecke, R. Blachnik and B. W. Tattershall, *Z. Anorg. Allg. Chem.*, 1994, **620**, 1115.
7 M. J. Frisch, G. W. Trucks, H. B. Schlegel, P. M. W. Gill, B. G. Johnson, M. A. Robb, J. R. Cheeseman, T. Keith, G. A. Petersson, J. A. Montgomery, K. Raghavachari, M. A. Al-Laham, V. G. Zakrzewski, J. V. Ortiz, J. B. Foresman, J. Cioslowski, B. B. Stefanov, A. Nanayakkara, M. Challacombe, C. Y. Peng, P. Y. Ayala, W. Chen, M. W. Wong, J. L. Andres, E. S. Replogle, R. Gomperts, R. L. Martin, D. J. Fox, J. S. Binkley, D. J. Defrees, J. Baker, J. P. Stewart, M. Head-Gordon, C. Gonzalez and J. A. Pople, GAUSSIAN 94, Revision E.2, Gaussian Inc., Pittsburgh, PA, 1995.
8 B. W. Tattershall, *J. Chem. Soc., Dalton Trans.*, 1987, 1515.
9 R. Blachnik, K. Hackmann and H.-P. Baldus, *Z. Naturforsch., Teil B*, 1991, **46**, 1165.
10 M. Baudler, R. Heumüller and K. Langerbeins, *Z. Anorg. Allg. Chem.*, 1984, **514**, 7.
11 A. R. Quirt, J. S. Martin and K. M. Worvill, NUMARIT, Version 771, SERC NMR Program Library, Daresbury, 1977.
12 Win-DAISY, Bruker-Franzen Analytik, Bremen, 1996.
13 Win-NMR 1D, Bruker-Franzen Analytik, Bremen, 1996.
14 A. Schäfer, H. Horn and R. Ahlrichs, *J. Chem. Phys.*, 1992, **97**, 2571.
15 A. Schäfer, C. Huber and R. Ahlrichs, *J. Chem. Phys.*, 1994, **100**, 5829.
16 B. W. Tattershall, E. L. Sandham and W. Clegg, *J. Chem. Soc., Dalton Trans.*, 1997, 81.
17 S. Böcker and M. Häser, *Z. Anorg. Allg. Chem.*, 1995, **621**, 258.
18 A. E. Reed, L. A. Curtiss and F. Weinhold, *Chem. Rev.*, 1988, **88**, 899.
19 H. O. Gavarini, M. A. Natiello and R. H. Contreras, *Theor. Chim. Acta*, 1985, **68**, 171.
20 H. M. McConnell, *J. Chem. Phys.*, 1956, **24**, 460.
21 J. A. Pople and D. P. Santry, *Mol. Phys.*, 1964, **8**, 1.
22 M. Kaupp, O. L. Malkina, V. G. Malkin and P. Pyykkö, *Chem. Eur. J.*, 1998, **4**, 118.
23 Extensible Computational Chemistry Environment Basis Set Database, Version 1.0, Molecular Science Computing Facility, Environmental and Molecular Sciences Laboratory, Richland, Washington, 1999. http://www.emsl.pnl.gov:2080/forms/basisform. html